Dalton Transactions

Accepted Manuscript

ROYAL SOCIETY OF CHEMISTRY

www.rsc.org/dalton

Electrochemical Performance and Biosensor Application of TiO_2 Nanotube Arrays with Mesoporous Structures Constructed by Chemical Etching

Jinwen Wang[1], Guangqing Xu[*1], Xu Zhang[1], Jun Lv[1], Xinyi Zhang[2], Zhixiang Zheng[1], Yucheng Wu[*1, 3]

1 Laboratory of Functional Nanomaterials and Devices, School of Materials Science and Engineering, Hefei University of Technology, Hefei 230009, China

2 School of Chemistry, Monash University, Clayton, VIC 3800, Australia

3 Anhui Provincial Key Laboratory of Advanced Functional Materials and Devices, Hefei University of Technology, Hefei 230009, China.

Abstract: Novel mesoporous TiO_2 nanotube arrays (TiO_2 NTAs) are synthesized by anodization method combined with chemical etching in HF solution, and the electrochemical performances are studied. Glucose oxidase (GOx) is immobilized on the mesoporous TiO_2 NTAs to achieve an efficient biosensor for amperometric detection of glucose. The morphology, structure, component and electrochemical performance of mesoporous TiO_2 NTAs are characterized by scanning electron microscope, high resolution transmission electron microscope, X-ray diffractometer, X-ray photoelectron spectrometer and electrochemical workstation, respectively. The influence of mesoporous structure on the electrochemical performance is discussed in detail by comparing the cyclic voltammograms and electrochemical impedance spectrum of TiO_2 and mesoporous TiO_2 NTAs in different conditions. High electrochemical active surface area and electron transfer rate play key roles on enhancing the electrochemical performance of mesoporous TiO_2 NTAs. When used as basis of biosensor, the amperometric response of glucose on GOx/TiO_2-0.5 NTAs electrode is linearly proportion to glucose concentration in the range from 0.1 to 6 mM with a sensitivity of 0.954 $\mu A \cdot mM^{-1} \cdot cm^{-2}$, which is 14.3 times that of un-etched GOx/TiO_2 NTAs.

Keywords: TiO_2 nanotube arrays; Mesoporous structure; Chemical etching; Electrochemistry; Biosensor

1 Introduction

TiO_2 is a common used semiconductor nanomaterial for many applications in environmental fields, including dye-sensitized solar cells [1, 2], water photoelectrolysis [3, 4] and photocatalytic degradation [5, 6] due to its high oxidizing activity of photogenerated holes, low cost, nontoxicity,

* Corresponding author: Tel.: +86 551 62901372
Email address: gqxu1979@hfut.edu.cn (Guangqing Xu)
ycwu@hfut.edu.cn (Yucheng Wu)

physical and chemical stability. Well aligned TiO_2 nanotube arrays (NTAs) were synthesized by Grimes via anodizing Ti sheets in HF solution [7]. The vertically oriented TiO_2 NTAs became a competing substrate in sensors, including gas sensor [8, 9], COD sensor [10, 11] and biosensor [12, 13], due to the special architecture of nanotube arrays.

The commercial biosensor, such as blood glucose meter, is composed of separate electrodes and enzymes, which requires consumption of enzyme in each determination, resulting in high use-cost. Immobilizing the enzymes on the electrode directly can solve this problem. Since Clark and Lyons first proposed the concept of a biosensor where an enzyme is incorporated on electrode surface [14], the immobilized biosensors have attracted great attentions.

Many nanomaterials have been employed as supports for immobilizing enzymes and developing enzyme-based biosensors. The immobilizing amount of enzymes, activity of immobilized enzymes and conductivity of the supports are the key factors for the sensitivity of biosensors. Well-organized TiO_2 NTAs possess good biocompatibility, environmental safety and large surface area. Also, TiO_2 NTAs are easy to coordinate with amine and carboxyl groups on the surface and act as an electron mediator, which facilitates the electron transfer between the redox centers of the enzymes and the electrode surface [15-17]. Thus, TiO_2 NTAs can be used as matrix to immobilize proteins and enzymes for biosensor. Xiao and co-workers reported the fabrication of TiO_2 NTAs by anodization of titanium foil for H_2O_2 biosensor design [18].

Many efforts have been devoted on the synthesis and modification of TiO_2 TNAs for enhancing the electrochemical performance of TiO_2 NTAs, such as metal nanoparticles modification (including Ag, Au and Pt) [19, 20], semiconductor quatum dots modification (including Cu_2O and CdS) [21, 22] and carbon nanostructures modification (including carbon nanotubes and graphene) [23, 24], which can provide better electron transportation and show an excellent capability to immobilize enzyme as well. In our previous work, TiO_2 NTAs based biosensors were synthesized and modified with Ag [25], Pt nanoparticles and graphene nanosheets [26]. The modification on TiO_2 nanotubes enhances the charger transfer between the electrolyte and the electrode, hence, enhance the detection performances of the biosensors. These efforts enhance the electrochemical performance of TiO_2 NTAs by external modification. The internal structure of TiO_2 nanotubes is the other key factor for electrochemical performances, including the crystal structure, geometric dimensioning and the surface condition. For example, the different exposed lattice planes of TiO_2 nanocrystals possess different catalytic reaction activity [27].

Great efforts have been dedicated to synthesize TiO_2 nanomaterials with controllable morphology

and porous structure [28]. In particular, mesoporous TiO_2 is a kind of attractive semiconductor allowing the reduction of various electron acceptors such as viologen, as well as electron transfer with biological molecules such as flavin coenzymes [29, 30]. Bao and co-workers first developed a novel TiO_2 with uniform porous structure via using multi-walled carbon nanotubes as template [31]. Serge Consier et al. for the first time described the functionalization of a mesoporous TiO_2 film immobilized with glucose oxidase for the amperometric detection of glucose [32].

In consideration that enzyme molecules contain lots of secondary branched structure, which requires extending room for maintaining its activity [33]. Mesopores on the nanotubes can act as cell to offer the required room. To our knowledge, the introduction of mesopores in TiO_2 NTAs, which is suitable for holding enzymes and accelerating charges transfer, has never been reported for biosensor application.

Here, TiO_2 NTAs with mesoporous structures were obtained by anodization method combined with chemical etching in HF solution. The mesoporous TiO_2 NTAs were immobilized with glucose oxidase (GOx) by physical adsorption and used for glucose determination.

2 Experimental

2.1 Chemicals and instruments

GOx was purchased from Sigma and used as received without further purification. Ethylene glycol (EG), hydrogen peroxide (H_2O_2), glucose, phosphate, ammonium fluoride (NH_4F), hydrogen fluoride (HF) and other reagents, were analytical reagent grade, and were purchased from Enterprise Group Chemical Reagent Co, LTD. Titanium foils (0.1 mm thickness, 99.6% purity) were purchased from Beijing Cuibolin Non-Ferrous Technology Developing Co. LTD and used as received.

A 0.05 M phosphate buffer solution (pH=7) containing Na_2HPO_4 and NaH_2PO_4 was used as supporting electrolyte. The enzyme solution was prepared by dissolving GOx in 0.05 M phosphate buffer solution (PBS) to make a 500 $U \cdot mL^{-1}$ solution and was kept at 4℃ in the fridge.

Anodization of TiO_2 NTAs was performed in a self-made electrolytic cell with a traditional two-electrode system (DH1722A-3). Morphologies of the as-prepared samples were observed with scanning electron microscope (SEM, SV8020) and high resolution transmission electron microscope (HRTEM, JEM-2100F). X-ray diffraction patterns of the samples were recorded at room temperature with 2θ angle ranging from 10 to 80° (XRD, D/MAX2500V). The existence valence of TiO_2 NTAs was determined by X-ray photoelectron spectrometer (XPS, CALAB250). Cyclic voltammetry and glucose detection were performed by an electrochemical workstation (CHI660D), comprising an

Ag/AgCl (3 M KCl) reference electrode, a Pt/Ti wire auxiliary electrode and a Pt disk working electrode fixed with as-prepared samples.

2.2 Synthetic procedure

Prior to the anodization, Ti foil was rinsed in ethanol and water with ultrasonic vibration for each 5 min. Ti foil was put into a two-electrode electrolytic cell as the working electrode, and a graphite electrode was used as the counter electrode with the distance of 2 cm. Anodic oxidation of Ti foil was performed in an EG solution containing 0.15 M NH_4F and 5% H_2O at a voltage of 60 V for 6 h. Then TiO_2 NTAs supported on Ti substrate were obtained and washed several times to remove the residual solution. The samples were ultrasonic vibrated in EG for 1 min to remove the debris covering on the top surface of TiO_2 NTAs. The dried TiO_2 NTAs were annealed in a muffle furnace at 500℃ for 2 h to get anatase TiO_2 NTAs.

The mesoporous structure of TiO_2 NTAs was constructed by chemical etching method in HF solution. The solutions with 0.2:10:89.8, 0.35:10:89.65, 0.5:10: 89.5 and 1:10: 89 volume ratio of HF, H_2O to EG were prepared respectively. Then 10 mL as-prepared solutions were transferred to teflon-lined stainless steel autoclave containing the anatase TiO_2 NTAs film inside. The autoclaves were then sealed and maintained at 100℃ for 5 h to complete the chemical etching process. Then TiO_2 NTAs film was cleaned in deionized water several times and dried at room temperature. The mesoporous TiO_2 NTAs prepared with different HF concentrations of 0.2%, 0.35%, 0.5% and 1% were defined as TiO_2-0.2, TiO_2-0.35, TiO_2-0.5 and TiO_2-1 NTAs, respectively.

The TiO_2 NTAs were fixed on the Pt disk electrode with silver conductive adhesive and a small cap, leaving a circular area of 0.2 cm^2 as working surface. GOx was immobilized on TiO_2 NTAs by physical adsorption method. In a typical procedure, 10 μL GOx solution with concentration of 500 $U \cdot mL^{-1}$ were dropped on the electrode. Then the electrode was left in the fridge at 4℃ overnight, following with immersion in buffer solution to remove the free GOx before electrochemical detection. The GOx/TiO_2 NTAs electrodes were then achieved and were stored at 4℃ in a fridge when not used.

2.3 Electrochemical test and glucose determination

The electrochemical properties of the as-prepared TiO_2 and mesoporous TiO_2 NTAs before and after GOx immobilization were characterized via cyclic voltammetry. The cyclic voltammetry testing was carried out in 0.05 M buffer solution, 10 mM H_2O_2 and 10 mM glucose at a scan rate of 10 mV/s. The amperometry determination of glucose was performed by successively injecting glucose with

different concentrations into 4 mL PBS, under constant stirring (100 rpm) at room temperature.

3 Results and discussion

3.1 Characterization of mesoporous TiO_2 NTAs

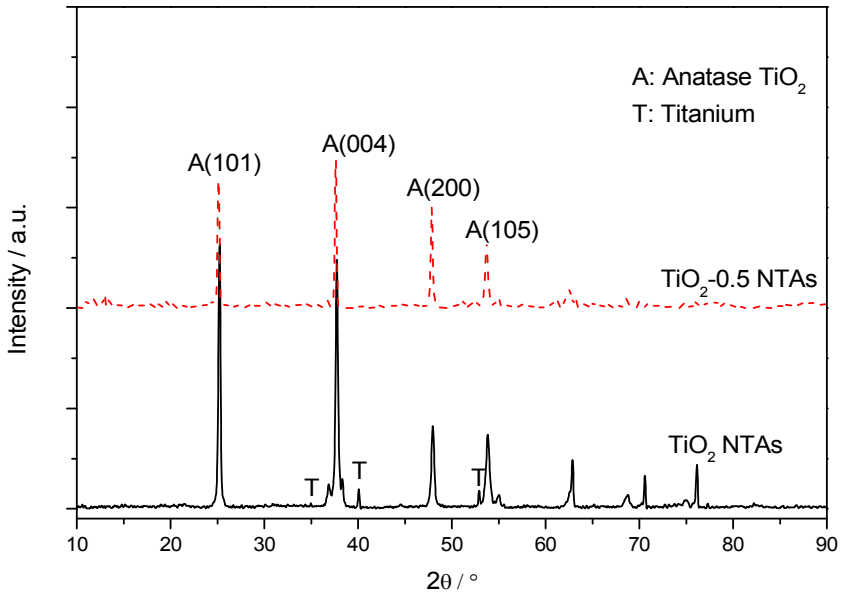

Fig.1 XRD patterns of TiO_2 NTAs and mesoporous TiO_2-0.5 NTAs

Fig.1 shows XRD patterns of TiO_2 NTAs before and after chemical etching. The anodized TiO_2 NTAs are in amorphous structure, which need to be crystalized by annealing method at 500℃ for 2 h. The diffraction peaks at 25.3° and 37.8° can be indexed to (101) and (004) lattice planes of anatase TiO_2, indicating that TiO_2 NTAs are in anatase structure. Some small peaks at 35.1°, 40.1° and 52.9° are the diffraction peaks of Ti substrate. The XRD pattern of mesoporous TiO_2-0.5 NTAs is almost the same with that of un-etched TiO_2 TNAs, indicating that the chemical etching process has no influence on the crystal structure of TiO_2 NTAs.

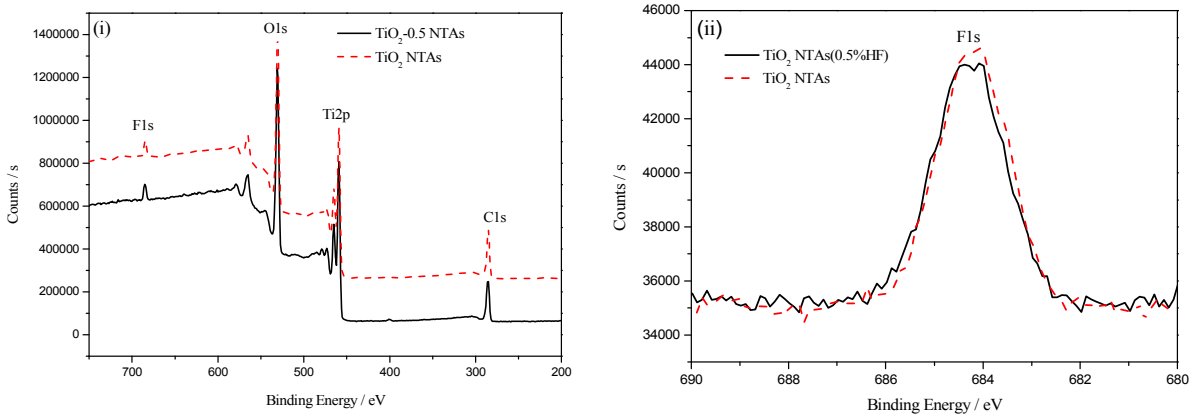

Fig.2 XPS patterns of as-prepared TiO_2 NTAs and mesoporous TiO_2-0.5 NTAs, (i) survey patterns, (ii) F 1s electron enlarged patterns

The commonly used XPS is applied to identify the elemental chemical state in TiO_2 NTAs and mesoporous TiO_2-0.5 NTAs, as shown in Fig.2. Fig.2 (i) shows the survey patterns of the two samples. The sharp peaks of O 1s and Ti 2p appeared at 530.02 eV and 458.45 eV are detected to confirm the major ingredients of the sample. Peak of C1s at 284.80 eV, existing in the sample, is originated from the testing process of XPS. Peak at 679.58 eV corresponding to F^- ions may originates from the anodization process or chemical etching process.

For further studying the state of F^- and making it clear whether F^- ions physically absorb on the surface or substitute in the crystal lattice of mesoporous TiO_2-0.5 NTAs, Fig.2 (ii) compares scan spectra of F1s between TiO_2 NTAs before and after etching. Two F1s peaks of TiO_2 and mesoporous TiO_2-0.5 NTAs are almost the same in intensity and binding energy, which are similar to the physically absorbed F^- on the surface of TiO_2 NTAs [34]. The similar state of the F^- ions on TiO_2 NTAs before and after etching confirms that F^- ions originate mainly from the anodization process.

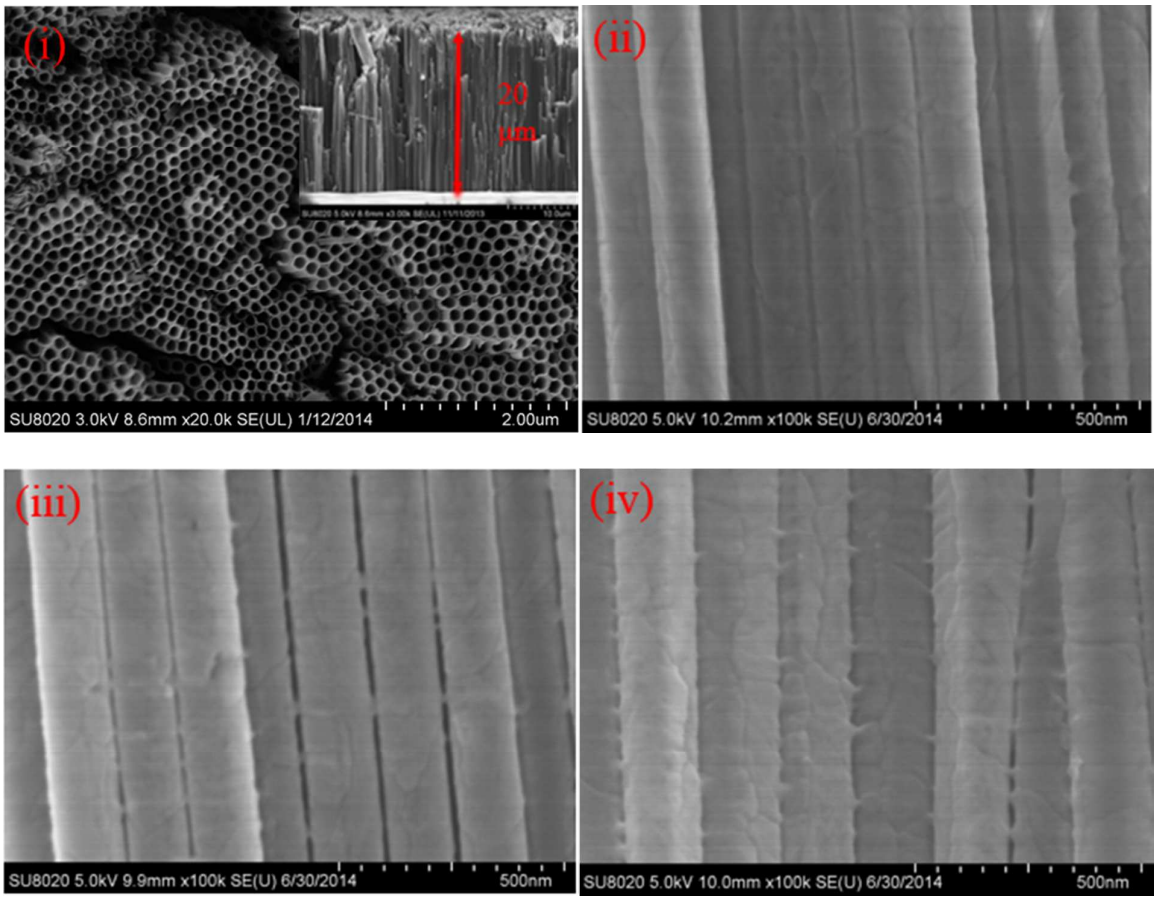

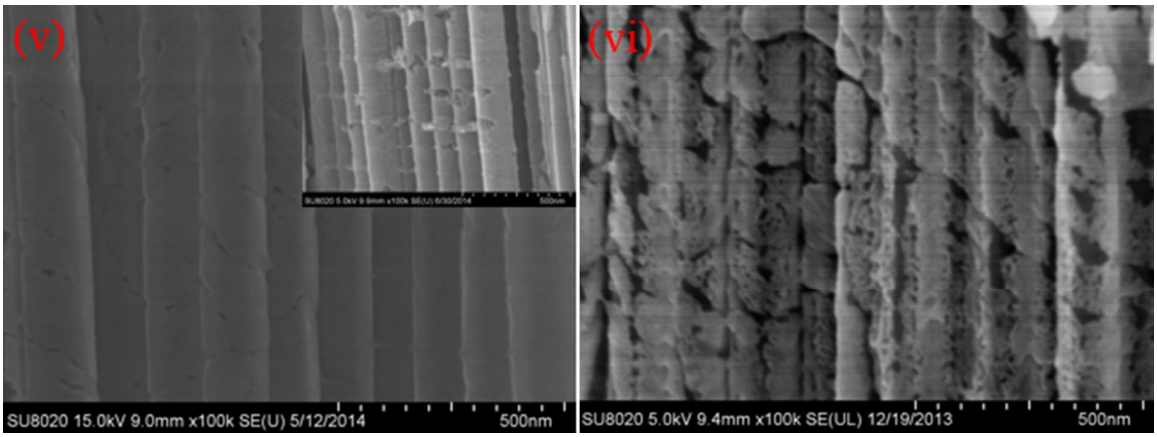

Fig.3 SEM morphologies of as-prepared TiO_2 NTAs (i, ii), mesoporous TiO_2-0.2 NTAs (iii), TiO_2-0.35 NTAs (iv), TiO_2-0.5 NTAs (v) and TiO_2-1 NTAs (vi)

Fig.3 shows SEM morphologies of TiO_2 and mesoporous TiO_2 NTAs prepared in HF solution with different concentrations. Fig.3 (i) is the top view of TiO_2 NTAs, from which the well aligned and closely packed TiO_2 nanotubes with the uniform tube diameter of 120 nm can be observed. It also can be observed in the profile view that the length is approximately 20 μm, as shown in the top right inset. The magnified profile views of TiO_2 and mesoporous TiO_2 NTAs are shown in Fig.3 (ii), (iii), (iv), (v) and (vi), respectively. No obvious mesopores on the tube walls of as-prepared TiO_2, mesoporous TiO_2-0.2 and TiO_2-0.35 NTAs can be observed in Fig.3(ii), (iii) and (iv). In consideration of the closely packed TiO_2 nanotubes, the inner surfaces of the nanotubes are the main sites of chemical etching. Only the mesopores through the tube walls can be observed in the outer surface of TiO_2 nanotubes. So when TiO_2 NTAs were etched in 0.5% HF solution, these mesopores can be observed in the outer walls of the nanotubes, as shown in Fig.3 (v), indicating the higher degree of chemical etching in higher HF concentration. Fig.3 (vi) also shows the morphology of mesoporous TiO_2-1 NTAs, in which large amount of mesopores distribute on the wall of the TiO_2 nanotubes. However, the severe destructing of the mesoporous TiO_2-1 NTAs make the film easily broken during the electrochemical test, and TiO_2-1 NTAs were not used in the further experiments.

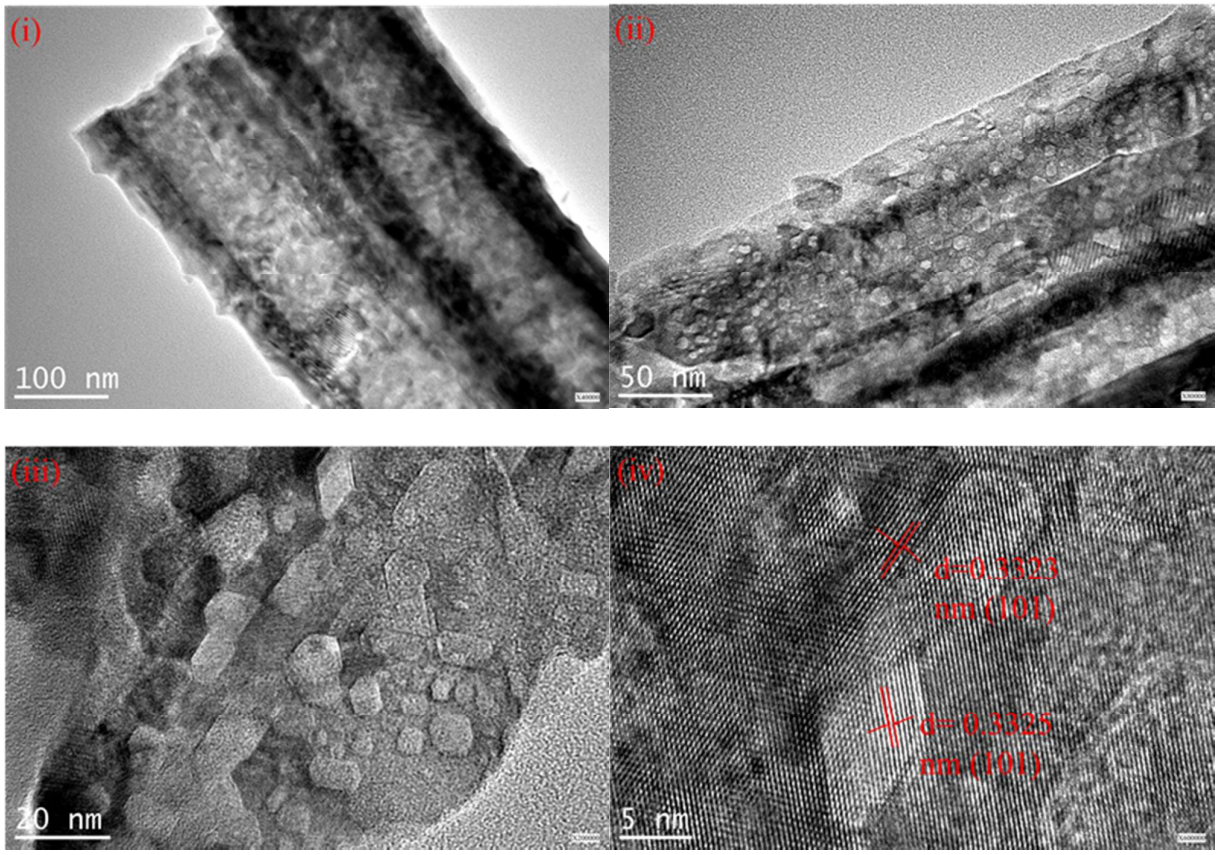

Fig.4 TEM morphologies of as-prepared TiO_2 NTAs and mesoporous TiO_2-0.5 NTAs, (i) as-prepared TiO_2 NTAs, (ii) mesoporous TiO_2-0.5 NTAs, (iii) mesoporous TiO_2-0.5 NTAs with higher magnification, (iv) HRTEM morphology of mesoporous TiO_2-0.5 NTAs

For further studying the inner structure of mesoporous TiO_2-0.5 NTAs, HRTEM tests are carried out, and the morphologies are shown in Fig.4. Fig.4 (i) shows the as-prepared TiO_2 nanotubes with the diameter of 120 nm, which corresponds to the morphology in Fig.3 (ii). Compared with TiO_2 nanotubes in fig.4 (i), there are lots of mesopores distributing in the walls of TiO_2 nanotubes after being etched, as shown in Fig.4 (ii). These mesopores are almost rectangle with size of above 10 nm with the sides parallel to the (101) plane of anatase TiO_2 as shown in Fig.4 (iii) and (iv). Mesopores are rectangle rather than sphere, which can be attributed to the (101) planes with relative low surface energy to minimize the overall surface energy, which has been confirmed by the fact that natural anantase crystal exposes (101) planes.

There are two kinds of surface species, Ti-OH_2^+ and Ti-OH on the surface of TiO_2 nanotubes, when anatase TiO_2 NTAs are put into the deionized water [35]. And the F^- ions addition converts surface species from Ti-OH_2^+ and Ti-OH to Ti-F. The corresponding surface reactions were considered as follows [36]:

$$Ti\text{-}OH_2^+ \rightarrow Ti\text{-}OH + H^+ \quad (1)$$

$$Ti\text{-}OH + H^+ + F^- \rightarrow Ti\text{-}F + H_2O \quad (2)$$

It is apparent that the adsorption of fluoride on TiO_2 replaces the surface hydroxyl groups to Ti-F species, and the chemical etching of anatase TiO_2 NTAs can be attributed to the production of TiF_4 in the hydrothermal condition.

3.2 Electrochemical performances of mesoporous TiO_2 TNAs

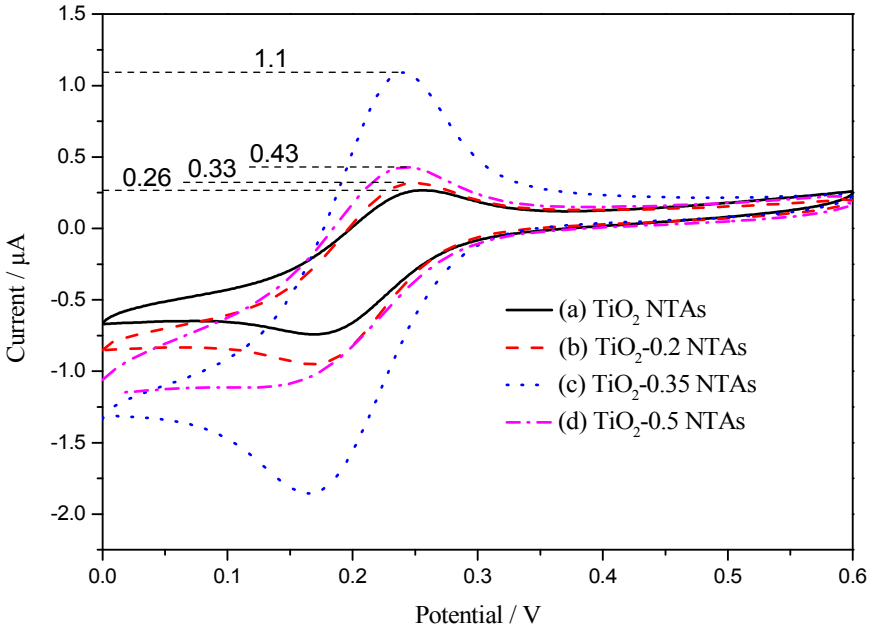

Fig.5 CVs of as-prepared TiO_2 NTAs, mesoporous TiO_2-0.2 NTAs, TiO_2-0.35 NTAs and TiO_2-0.5 NTAs in an aqueous solution containing 10 mM $K_3[Fe(CN)_6]$ and 0.1 M KCl

Fig.5 shows typical cyclic voltammograms (CVs) of TiO_2 and mesoporous TiO_2 NTAs in the electrolyte containing 10 mM $K_3[Fe(CN)_6]$ and 0.1 M KCl. A pair of redox peaks can be observed for TiO_2 and mesoporous TiO_2 NTAs at the potentials ranging from 0 to 0.6 V due to the oxidation and reduction of $[Fe(CN)_6]^{3-}$ ions.

For a reversible process, Randles-Sevick Equation is applicable. Therefore, the electrochemical active surface areas of TiO_2 NTAs and mesoporous TiO_2 NTAs can be determined by equation (3).

$$I_p = (2.69\times10^5)n^{3/2}AD_0^{1/2}v^{1/2}C_0^* \quad (3)$$

Where I_p is the peak current, n is the number of electrodes, A is the electrochemical effective surface area of the electrode (in cm^2), C_0^* is the concentration (in mol/cm^3), D_0 is the diffusion coefficient (in

cm^2/s) and v is the scan rate (in V/s). The peak current (I_p) corresponds to the electrochemical effective surface area (A) of the electrodes.

All mesoporous TiO_2 NTAs exhibit higher peak intensities and larger capacitance than that of as-prepared TiO_2 NTAs, indicating that mesoporous TiO_2 NTAs possess larger electrochemical active surface areas. The peak current increases with the increase of HF concentration ranging from 0.2% to 0.35% and achieves the maximum of 1.1 μA in the HF concentration of 0.35%. Further increase of the concentration to 0.5% will decrease the peak current to 0.43 μA. The change of the peak currents corresponds to the change of the electrochemical active surface area, that is, the mesoporous TiO_2-0.35 NTAs possess the biggest electrochemical active surface area.

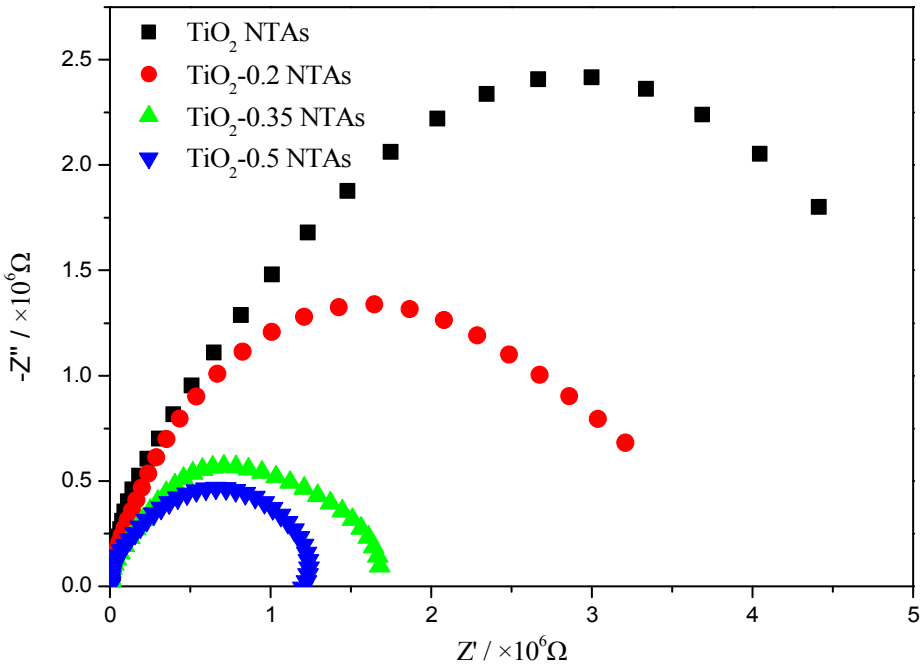

Fig.6 EISs of as-prepared TiO_2 NTAs, mesoporous TiO_2-0.2 NTAs, TiO_2-0.35 NTAs and TiO_2-0.5 NTAs in buffer solution

Electrochemical impedance spectrum (EIS) is used to investigate the electrode process and the diffusion kinetics as well as mass parameter. The semicircle part of the Nyquist plot gives the information about capacitive and resistance, and the linear part shows the diffusion effects. The semicircle diameter at higher frequencies corresponds to the charge transfer resistance (R_{ct}), and the linear part at lower frequencies corresponds to the diffusion process.

Fig.6 exhibits EIS plots of different electrodes in the frequency range from 10^{-2} to 10^5 Hz at potential of 0.1 V. The electrodes exhibit almost straight lines in the lower frequencies which

corresponds to the diffusion process. The R_{ct} of mesoporous TiO_2 NTAs is lower than that of as-prepared TiO_2 NTAs, and decrease with the increase of HF solution, which means that the mesoporous TiO_2 NTAs possess higher electron transfer rate than that of un-etched TiO_2 NTAs. The electron transfer rate of mesoporous TiO_2 NTAs increases with the concentration ranging from 0.2% to 0.5%, which is different with the trends of the electrochemical active surface area.

In consideration that the quantification of glucose is based on the electrochemical detection of the enzymatically liberated H_2O_2, the electrochemical response to H_2O_2 of the electrode is a key factor for the sensor's sensitivity. High catalytic efficiency to H_2O_2 is benefit to achieve high sensitivity toward glucose. Here, H_2O_2 is used as a probe to determine the catalytic property of different TiO_2 NTAs electrodes.

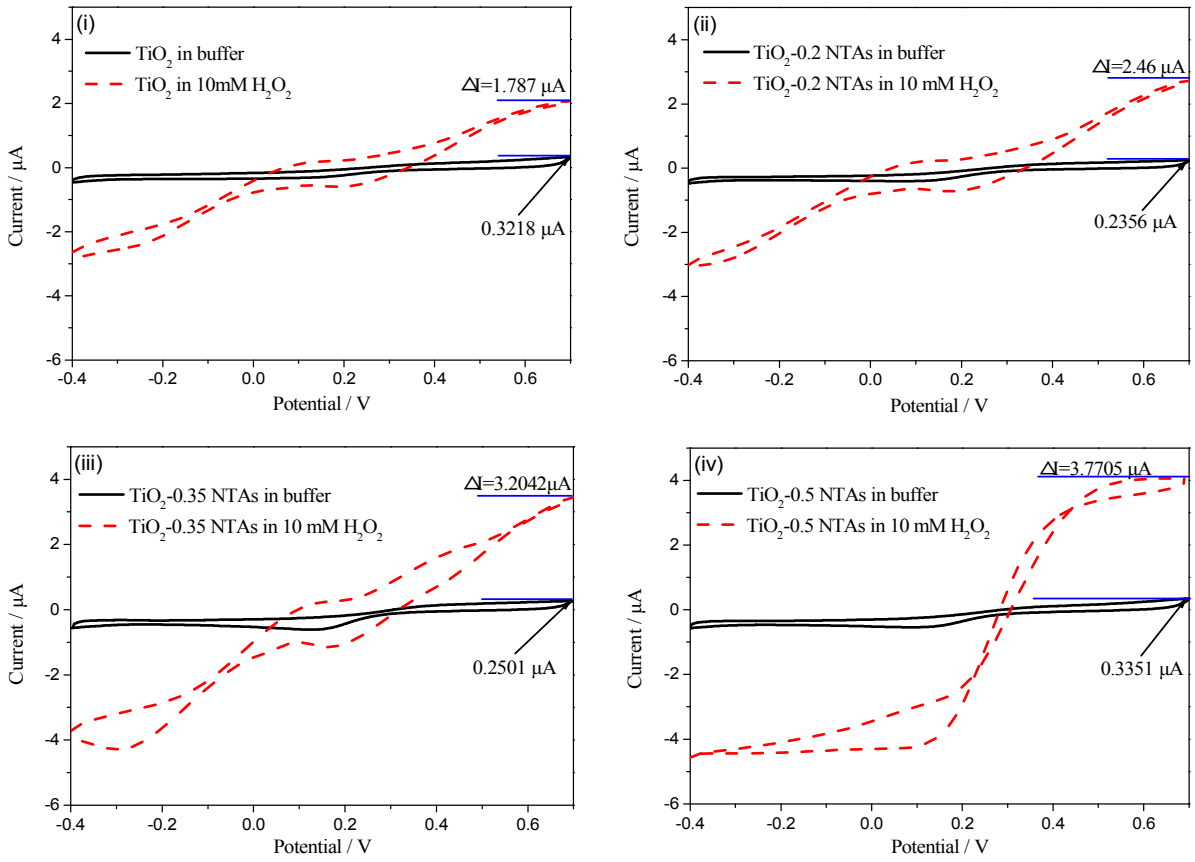

Fig.7 CVs of as-prepared TiO_2 NTAs (i), mesoporous TiO_2-0.2 NTAs (ii), TiO_2-0.35 NTAs (iii) and TiO_2-0.5 NTAs (iv) in buffer solution in absence and presence of 10 mM H_2O_2

Fig.7 shows the CVs of as-prepared TiO_2 NTAs(i), mesoporous TiO_2-0.2 (ii), TiO_2-0.35 (iii), and TiO_2-0.5 (iv) NTAs in buffer solution without and with 10 mM H_2O_2 at the scan rate of 10 mV/s. When H_2O_2 is added in buffer solution, additional anodic and cathodic currents can be obtained due

to the H_2O_2 oxidation and reduction on TiO_2 NTAs. Fig.7 (i) shows the comparison of CVs obtained on TiO_2 TNAs in buffer and in 10 mM H_2O_2 solutions, from which the anodic current increment of 1.787 μA at 0.7 V can be observed. All the mesoporous TiO_2 NTAs possess higher current responses than that of un-etched TiO_2 NTAs, such as 2.46, 3.204 and 3.771 μA for TiO_2-0.2 (ii), TiO_2-0.35 (iii), and TiO_2-0.5 (iv) NTAs respectively. The higher current increments of mesoporous TiO_2 NTAs indicates better catalytic efficiency of H_2O_2 oxidation.

In addition, the maximum current response for H_2O_2 oxidation is achieved by TiO_2-0.5 NTAs, which is consistent with the EIS results in Fig.6, indicating that the best electron transfer ability induces the highest electrocatalytic efficiency of H_2O_2.

3.3 CVs of mesoporous GOx/TiO_2 NTAs

GOx was immobilized on TiO_2 and mesoporous TiO_2 NTAs by physical adsorption to achieve glucose biosensor, and defined as GOx/TiO_2 NTAs. In general, biosensor enzymes are immobilized on the sensors by either cross-linking with glutaraldehyde or being protected with a thin layer of Nafion to prevent the enzymes from losing. Here, the nanotubular structure of TiO_2 NTAs and the highly dispersible mesopores in the tube walls provide a suitable structure for immobilization of GOx. The CVs of TiO_2 and mesoporous TiO_2 NTAs before and after being immobilized with GOx in buffer solution in absence and presence of 10 mM glucose are shown in Fig.8.

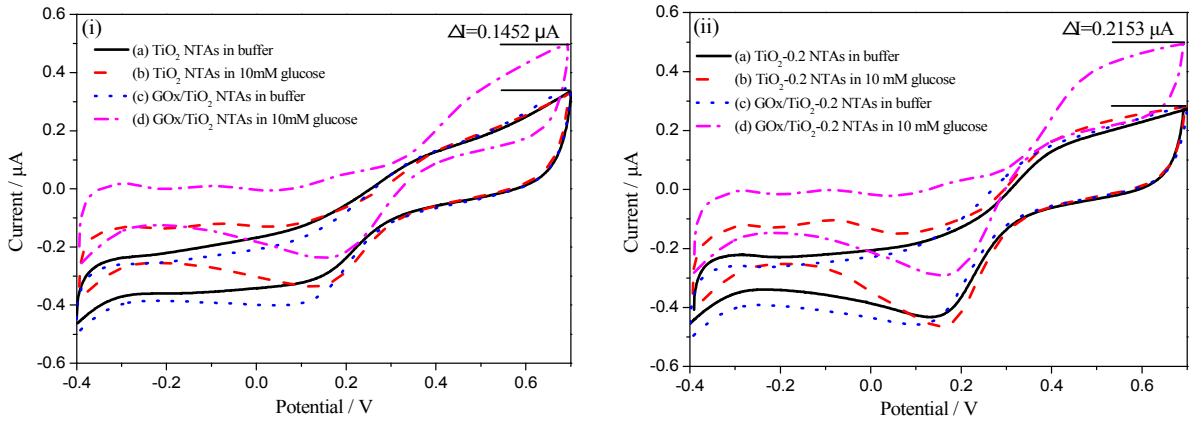

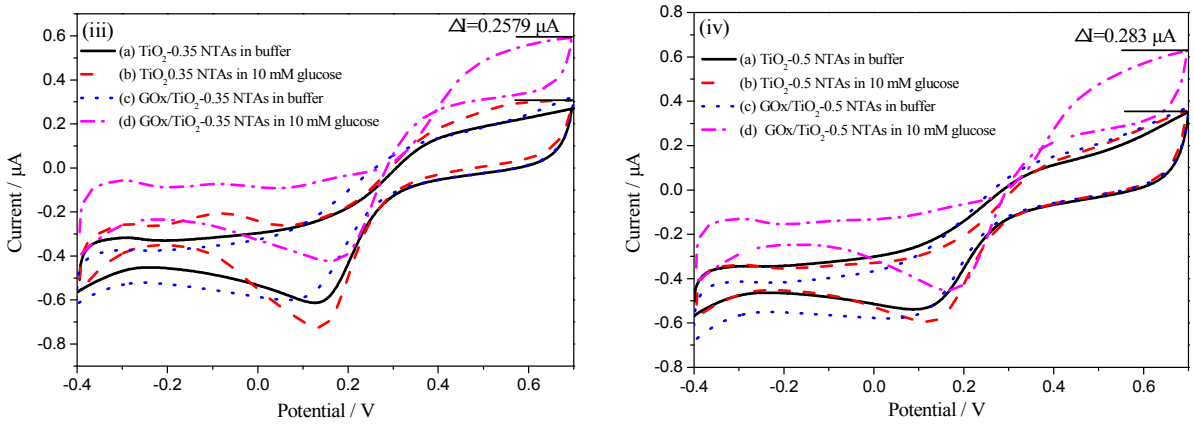

Fig.8 CVs of as-prepared TiO_2 NTAs and mesoporous TiO_2 NTAs before and after being immobilized with GOx in buffer solution in absence and in presence of 10 mM glucose, TiO_2 NTAs (i), TiO_2-0.2 NTAs (ii), TiO_2-0.35 NTAs (iii), TiO_2-0.5 NTAs (iv)

Fig.8 (i) shows the CVs of as-prepared TiO_2 NTAs in different conditions. Curve (a) and (b) compare the CVs of TiO_2 NTAs in buffer and in 10 mM glucose. Similarity of the two curves indicates that there is no electrochemical activity of TiO_2 NTAs for glucose oxidation in the testing potential region. When GOx is immobilized on TiO_2 NTAs, the obvious current response in positive potentials can be observed, as being compared in curve (c) and (d). The current increment at potential of 0.7 V is 0.145 μA. The cathodic currents at low potentials decrease in glucose solution compared with that in buffer, indicating that cathodic current response cannot be used for glucose determination.

Fig.8 (ii), Fig.8 (iii) and Fig.8 (iv) show the CVs of mesoporous TiO_2-0.2, TiO_2-0.35 and TiO_2-0.5 NTAs in different conditions. Similar with TiO_2 NTAs, the mesoporous TiO_2 NTAs possess no activity of direct electrochemical oxidation of glucose. After being immobilized with GOx, anodic current responses of 0.215, 0.258 and 0.283 μA at 0.7 V can be obtained, which are higher than that of as-prepared TiO_2 NTAs. Also, the current response to 10 mM glucose increase with the HF concentration ranging from 0.2% to 0.5%, corresponding to the electrocatalytic efficiencies of H_2O_2 in Fig.7.

3.4 Glucose determination

To evaluate the sensitivity of as-prepared biosensors based on TiO_2 NTAs and mesoporous TiO_2 NTAs, the typical current responses of the obtained biosensors (GOx/TiO_2 and mesoporous GOx/TiO_2 TNAs) were determined by amperometry. When the background current in buffer solution is steady, the glucose solution with certain concentration is injected into the buffer solution and the

current response is carried out. All processes are under continuous stirring (100 rpm) condition with an applied potential of 0.7 V, and the results are shown in Fig.9.

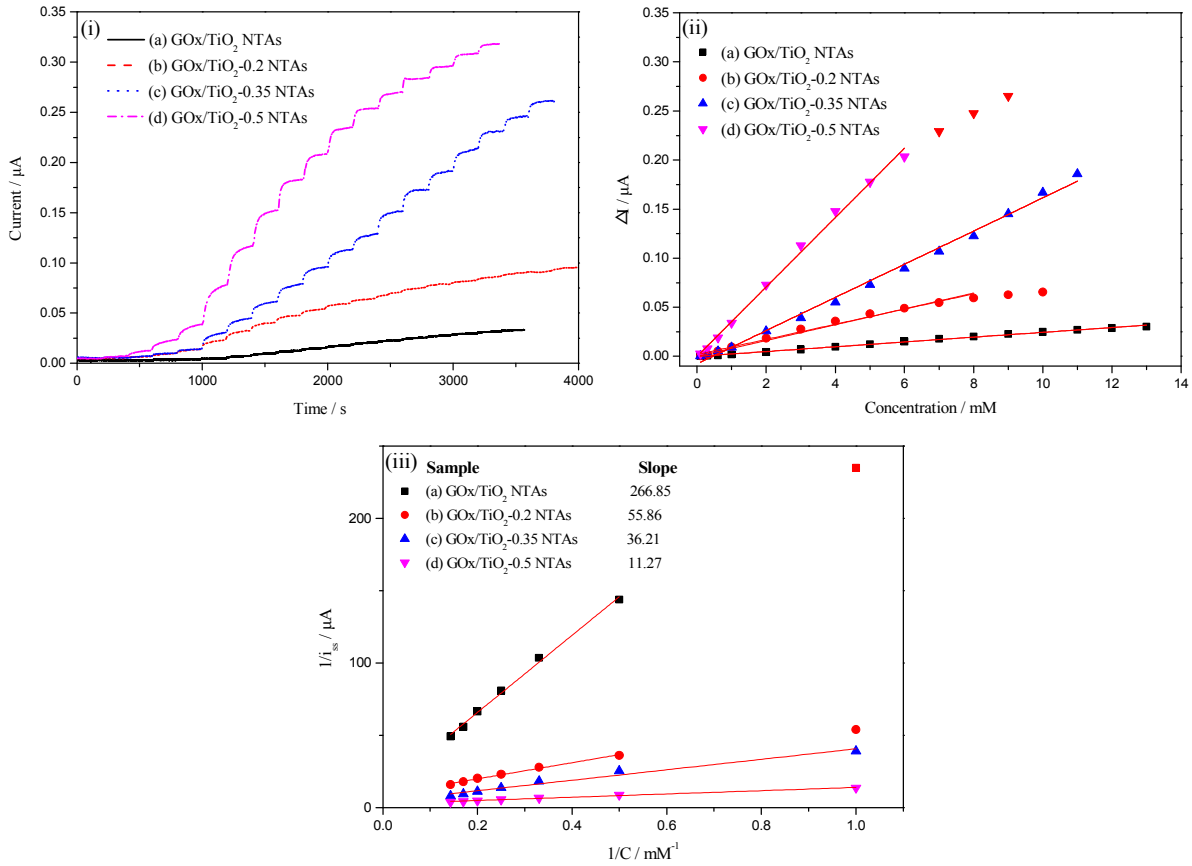

Fig.9 Amperometric determination of glucose by GOx/TiO_2 NTAs, GOx/TiO_2-0.2 NTAs, GOx/TiO_2-0.35 NTAs, GOx/TiO_2-0.5 NTAs electrodes. (i) Current responses with successive injection of glucose; (ii) Calibration curves; (iii) Lineweaver-Burk-type plots for electrochemical determination of apparent Michaelis-Menten constants

From the comparison of current-time curves in Fig.9 (i), GOx/TiO_2 NTAs (curve (a)) show considerably weak response for glucose injection at the applied potential of 0.7 V, while all mesoprous GOx/TiO_2 NTAs possess higher current response than that of GOx/TiO_2 NTAs. The current response to glucose increases with the HF concentration and achieve the maximum in GOx/TiO_2-0.5 NTAs. The calibration plots between the current change and glucose concentration are show in Fig.9 (ii), which can give the determination parameters of these biosensors. The slopes obtained by linear fitting of the data show the sensitivities of the biosensors. The sensitivity of TiO_2 NTAs is 0.066 $\mu A \cdot mM^{-1} \cdot cm^{-2}$ (calculated with slope of 0.00246 $\mu A \cdot mM^{-1}$ and working area of 0.037 cm^2) with linear range from 0.1 to 13 mM. The sensitivity of GOx/TiO_2-0.5 NTAs is 0.954 $\mu A \cdot mM^{-1} \cdot cm^{-2}$ in the linear range from 0.1 to 6 mM, which is twice that of GOx/TiO_2-0.35 NTAs, 4.8

times that of GOx/TiO_2-0.2 NTAs and 14.3 times that of GOx/TiO_2 NTAs.

The effect of mesopores on the sensitivity enhancement can be seen in the kinetics data on the enzyme reaction. The apparent Michalis-Menen constants, K_m, for immobilized GOx can be determined electrochemically by using the modified Linewearer-Burk equation.

$$1/i_{ss} = \left(K_m/i_{mas}\right)\left(1/C\right) + 1/i_{max} \quad (4)$$

Where i_{max} and i_{ss} are the currents measured for enzymatic product detection under conditions of saturation and steady state for given substrate concentration C. A plot of $1/i_{ss}$ vs 1/C will give a straight line with the slope equal to K_m/i_{max} and intercept equal to $1/i_{max}$, as shown in Fig.9 (iii). The lower K_m means the better catalytic action of GOx. The K_m values of GOx/TiO_2 NTAs is higher than that of GOx/ TiO_2-0.5 NTAs. The K_m is affected by two factors, mass diffusion limitation and the reaction kinetics of GOx. Generally, the effect of the two factors cannot be separated in the electrochemical method. At high rotation speed (ω> 1600 rpm) the enzyme operates under catalysis control [37] On the electrode immobilized with GOx, assuming that the mesopores do not have effect on the intrinsic catalysis property of GOx, the difference of K_m can be attributed to the mass diffusion limitation of O_2 and H_2O_2 through the mesopores. The higher porosity of TiO_2-0.5 NTAs shows a higher mass diffusion rate than that of TiO_2 NTAs.

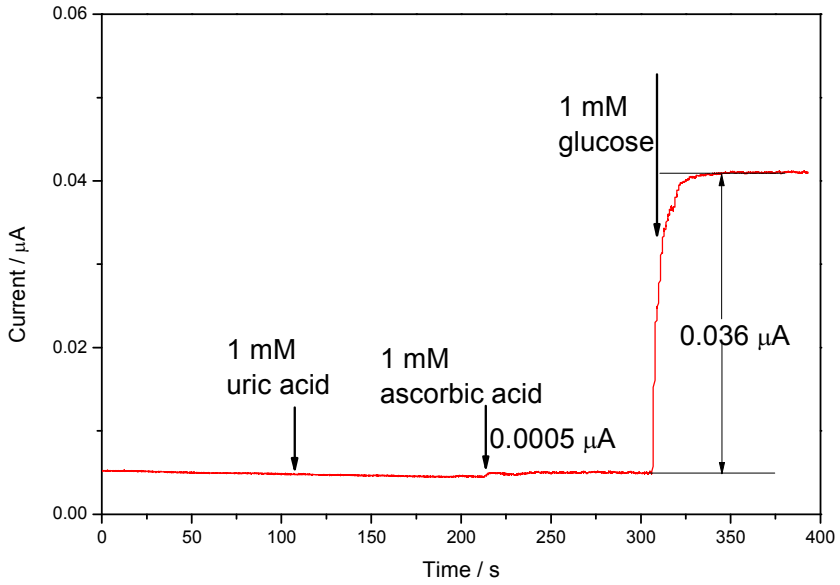

Fig.10 Selectivity test of GOx/ TiO_2-0.5 NTAs electrode with additions of 1 mM uric acid, 1 mM ascorbic acid and 1 mM glucose

Selectivity of this biosensor was investigated by testing the amperometric response with injections

of 1 mM uric acid, 1 mM ascorbic acid and 1 mM glucose, in which the previous two components are among the potential interfering electroactive species, as shown in Fig.10. 1 mM uric acid did not give any observable current response. And 1 mM ascorbic acid gave a response of 0.0005 μA, which is 1.39% to the current response of 1 mM glucose (0.036 μA), indicating a good selectivity of the biosensor.

To detect the stability of the GOx/ TiO_2-0.5 NTAs electrode, CVs of the electrode in 10 mM glucose solution were performed for 20 circles, as being shown in Fig.11. The CVs of the electrode in buffer solution are also listed in this figure for comparison. The current response is 0.283 μA for the first circle and 0.265 μA for the last circle. Only 6.36% response loss indicates the excellent stability of the GOx/TiO_2-0.5 NTAs electrode.

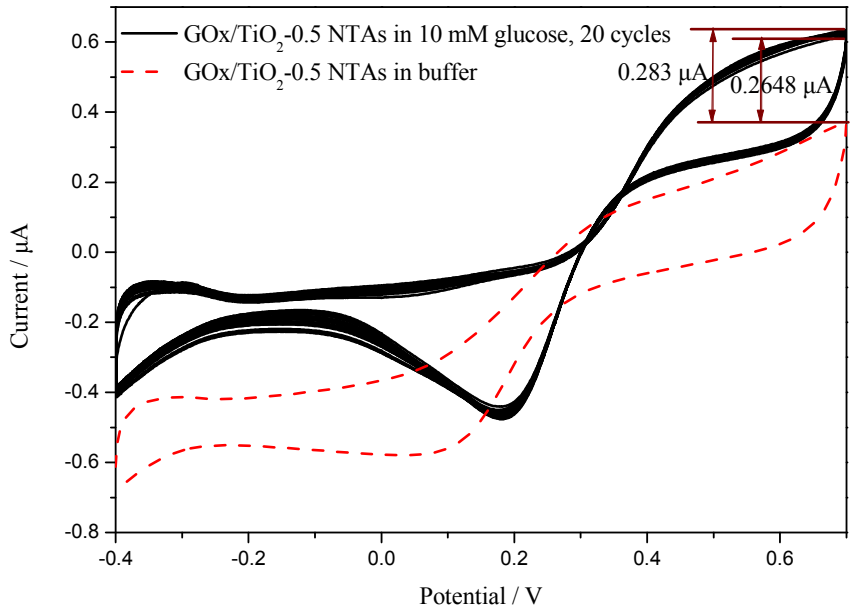

Fig.11 CVs of GOx/TiO_2-0.5 NTAs in buffer solution and in 10 mM glucose solution for 20 cycles

3.5 Mechanism discussion

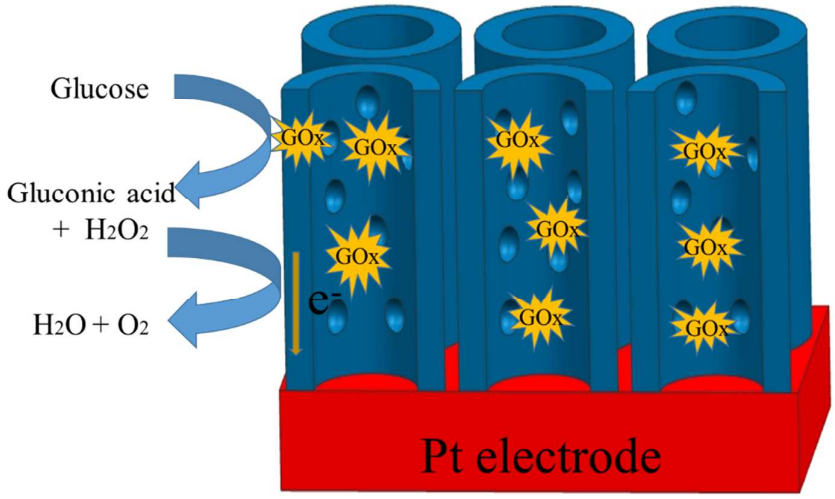

Fig.12 Schematic diagram of glucose detection on mesoporous GOx/TiO_2 NTAs

XPS results in Fig.3 have confirmed the similarity of the F^- ions in TiO_2 NTAs before and after being etched, which indicates that enhancements of the electrochemical performances after chemical etching are induced by the mesoporous structure instead of the absorbed F^- ions. The mesoporous structure of TiO_2 NTAs constructed by chemical etching method can enhance the electrochemical performances, hence, enhance the current response to glucose. The excellent sensitivity can be attributed to mesoporous structure of TiO_2 NTAs by the synergetic effects of providing more electrochemical active surface area and higher electron transfer rate. The schematic diagram of glucose detection on mesoporous GOx/TiO_2 NTAs is shown in Fig.12.

The catalytic oxidation of glucose based on the immobilized GOx can be explained as follows:

$$\text{Glucose} + O_2 \xrightarrow{GOx} \text{Gluconic acid} + H_2O_2 \qquad (5)$$

In other words, chemical reaction of glucose with GOx is the first step of glucose determination, which produces H_2O_2 in the presence of dissolved oxygen. The enzymatic reaction requires abundant dissolved oxygen and large amount of active enzymes.

In consideration that the scale of mesopores about 10 nm is similar to that of GOx, the extending room is benefit for immobilizing enzymes and maintaining its activity. The active surface available for enzymes immobilizing is enhanced due to the increase of surface area resulting from the mesoporous structure [38]. That is, the mesoporous structure can offer high enzymes loading without serious loss of activity, meeting the requirements of the first step well.

The second step of glucose determination is obtaining the current response of H_2O_2 liberated by enzymatic reaction by the following reaction:

$$H_2O_2 \rightarrow O_2 + 2H^+ + 2e^- \quad \text{(anodic response)} \qquad (6)$$

The electrocatalytic oxidation of H_2O_2 takes place on the electrode when applying positive potential, and the anodic current response corresponding to H_2O_2 concentration can be obtained. Hence, high electrochemical activity to H_2O_2 oxidation is benefit for the electrodes achieving high current response to glucose. The CVs in Fig.7 have confirmed that mesoporous TiO_2 NTAs possess higher current response to H_2O_2, meeting the requirement of the second step of glucose detection.

One thing should be noted is the effects of electrochemical active surface area and electron transfer rate on the electrochemical oxidation of H_2O_2. Fig.5 and Fig.6 confirm that mesoporous TiO_2 NTAs possess higher electrochemical active surface area and electron transfer rate than that of un-etched TiO_2 NTAs respectively. However, the highest surface area appears in TiO_2-0.3 NTAs, and the highest electron transfer rate in TiO_2-0.5 NTAs. Higher current response to H_2O_2 of TiO_2-0.5 NTAs than that of TiO_2-0.3 NTAs (shown in Fig.7) indicates the electron transfer rate plays more important role in the electrochemical process of H_2O_2 oxidation. Also, twice glucose sensitivity of GOx/TiO_2-0.5 NTAs to GOx/TiO_2-0.3 NTAs confirms this result.

4 Conclusions

In this work, mesoporous TiO_2 NTAs are successfully synthesized by chemical etching in HF solution and used as basis of biosensor for glucose determination. Effect of HF concentration on the mesoporous structure and electrochemical activity are also discussed. Mesopores with rectangle shape on TiO_2 nanotubes enhance the electrochemical active surface area and electron transfer rate of TiO_2 NTAs. And the electron transfer rate plays more important role than active surface area in sensitivity of the biosensor. Mesoporous TiO_2-0.5 NTAs immobilized with GOx possess the maximum sensitivity of 0.954 $\mu A \cdot mM^{-1} \cdot cm^{-2}$ with linear range from 0.1 to 6 mM, which is 14.3 times that of un-etched GOx/TiO_2 NTAs.

Acknowledgement

This work was supported by Nature Science Foundation of China (51102071, 51172059 and 51272063), Fundamental Research Funds for the Central Universities (2013HGQC0005), and Nature Science Foundation of Anhui Provience (1408085QE86).

References

[1] G.K. Mor, K. Shankar, M. Paulose, O.K. Varghese, C.A. Grimes, *Nano Lett.*, 2006, 6, 215.

[2] U. Bach, D. Lupo, P. Comte, J. E. Moser, F. Weissortel, J. Salbeck, H. Spreitzer, M. Gratzel, *Nature* 1998, 359, 583.

[3] M. Ni, M.K.H. Leung, D.Y.C. Leung, K. Sumathy, *Renew. Suntain. Ener. Rev.*, 2007, 11, 401.

[4] J.H. Park, S. Kim, A.J. Bard, *Nano Lett*, 2006, 6, 24.

[5] Y. Kuwahara, H. Yamashita, *J. Mater. Chem.*, 2011, 21, 2047.

[6] H. Chen, D. Li, X. Li, J. Li, Q. Chen, B. Zhou, *J. Solid State Eletrochem.*, 2012, 16, 3907.

[7] V. Zwilling, M. Aucouturier, E. Darque-Ceretti, *Electrochim. Acta*, 1999, 45, 921.

[8] O.K. Varghese, D. Gong, M. Paulose, K.G. Ong, C.A. Grimes, *Sensor. Actuat. B-Chem.*, 2003, 93, 338.

[9] J. Gong, Y. Li, Z. Hu, Z. Zhou, Y. Deng, *J. Phys. Chem. C*, 2010, 114, 9970.

[10] Q. Zheng, B. Zhou, J. Bai, L. Li, Z. Jin, J. Zhang, X. Zhu, *Adv. Mater.*, 2008, 20, 1044.

[11] H.P. Liu, G.Q. Xu, J.W. Wang, J. Lv, Z.X. Zheng and Y.C Wu, *Electrochim. Acta*, 2014, 130, 213.

[12] H. Cao, Y. Zhu, L. Tang, X. Yang, C. Li, *Electroanal.*, 2008, 20, 2223.

[13] K.S. Mun, S.D. Alvarez, W.Y. Choi, M.J. Sailor, *Acs Nano*, 2010, 4, 2070.

[14] L.C. Clark, C. Lyons, *Ann NY. Acad. Sci.*, 1962, 102, 29.

[15] X. Cui, C.M. Hui, J. Zang, S. Yu, *Biosens. Bioelectron.*, 2007,22, 3288.

[16] J. Zang, C.M. Li, X. Cui, J. Wang, X. Sun, H. Dong, C.Q. Sun, *Electroanal.*, 2007, 19, 1008.

[17] C.M. Li, C.S. Cha, Front. *Biosci-Landmark.*, 2004, 9, 3479.

[18] P. Xiao, B. B. Garcia, Q. Guo, D. Liu, G. Cao, *Electrochem. Commun.*, 2007, 9, 2441.

[19] S.F. Chen, J.P. Li, K. Qian, W.P. Xu, Y. Lu, W.X. Huang, S.H. Yu, *Nano Res.*, 2010, 3, 244.

[20] B. Xin, L. Jing, Z. Ren, B. Wang, H. Fu, *J. Phys. Chem. B*, 2005, 109, 2805.

[21] Y. Hou, X. Li, X. Zou, X. Quan, G. Chen, *Environ. Sci. tech.*, 2008, 43, 858.

[22] X.F. Gao, W.T. Sun, Z.D. Hu, G. Ai, Y.L. Zhang, S. Feng, L.M. Peng, *J. Phys. Chem. C*, 2009, *113*, 20481.

[23] H. Yu, X. Quan, S. Chen, H. Zhao, *J. Phys. Chem. C*, 2007, *111*, 12987.

[24] P. Song, X. Zhang, M. Sun, X. Cui, Y. Lin, *Nanoscale*, 2012, 4, 1800.

[25] C.X. Feng, G.Q. Xu, H.P. Liu, J. Lv, Z.X. Zheng, Y.C Wu, *J. Solid State Electrochem.*, 2014, 18, 163.

[26] C.X. Feng, G.Q. Xu, H.P. Liu, J. Lv, Z.X. Zheng, Y.C Wu, *J. Electrochem. Soc.*, 2014, 161, B1.

[27] J.S. Chen, Y.L. Tan, C.M. Li, Y.L. Cheah, D. Luan, S. Madhavi, X.W. Lou, *J. Am. Chem. Soc.*, 2010, 132, 6124.

[28] S.J. Bao, Q.L. Bao, C.M. Li, Z.L. Dong, *Electrochem. Commun.*, 2007, 9, 1233.

[29] Z. Yang, Y. Tang, J. Li, Y. Zhang, X. Hu, *Biosens. Bioelectron.*, 2014,54, 528.

[30] J. Moser, M. Gratzel, *J. Am. Chem. Soc.*, 1983, 105, 6547.

[31] S.J. Bao, C.M. Li, J.F. Zang, X.Q. Cui, Y. Qiao, J. Guo, *Adv. Funct. Mater.*, 2008, 18, 591.

[32] S. Consnier, C. Gondran, A. Senillou, M. Gratzel, N. Vlachopoulos, *Electroanal.*, 1997, 9, 1387.

[33] Q. Chi, J. Zhang, S. Dong, E. Wang, *J. Chem. Soc.*, *Faraday Trans.*, 1994, 90, 2057.

[34] G. Wu, J. Wang, D.F. Thomas, A. Chen, *Langmuir*, 2008, 24, 3503.

[35] P.A. Connor, K.D. Dobson, A.J. Mcquillan, *Langmuir*, 1999, 15, 2402

[36] M.S. Vohra, S. Kim, W. Choi, *J. Photochem. Photobio. A: Chem*., 2003, 160, 55.

[37] R.A. Kamin, G.S. Wilson, *Analy. Chem.*, 1980, 52, 1198.

[38] D. Lee, J. Lee, J. Kim, J. Kim, H.B. Na, B. Kim, C.H. Shin, J.H. Kwak, A. Dohnalkova, J.W. Grate, T. Hyeon, H.S. Kim, *Adv. Mater.*, 2005, 17, 2828.

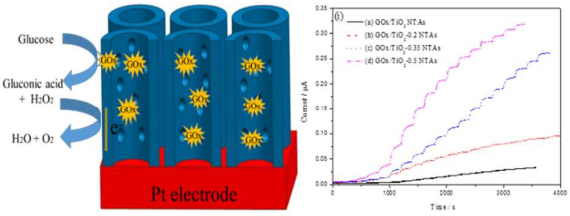

Novel mesoporous structures on TiO_2 nanotube arrays are achieved for enhancing the electrochemical performances.